

Microscopic systems with and without Coulomb interaction, fragmentation and phase transitions in finite nuclei

J.M. Carmona^{1a}, J. Richert^{2b}, and P. Wagner^{3c}

¹ Dipartimento di Fisica dell'Università and INFN, I-56127 Pisa, Italy

² Laboratoire de Physique Théorique, Université Louis Pasteur,
 3, rue de l'Université, 67084 Strasbourg Cedex (France) - UMR 7085

³ Institut de Recherches Subatomiques, BP28, 67037 Strasbourg Cedex 2 (France) - UMR 7500

December 2, 2024

Abstract. We test the influence of the Coulomb interaction on the thermodynamic and cluster generation properties of a system of classical particles described by different lattice models. Numerical simulations show that the Coulomb interaction produces essentially a shift in temperature of quantities like the specific heat but not qualitative changes. We also consider a cellular model. The thermodynamic properties of the system are qualitatively unaltered.

PACS. 05.70Ce, 64.60Cn Thermodynamics of finite systems. Lattice models. Cellular model. Coulomb interaction.

1 Introduction

In the recent past the success of percolation models [1] and their link with other generic approaches like Ising and Potts [2, 3] has led to the development of many lattice models [4–11] which were used as sensible albeit schematic descriptions of excited disassembling nuclei. As simple as

they may appear, their thermodynamic properties were considered as being at least qualitatively those of bound nucleon systems which interact essentially by means of the short range nuclear interaction. It was tacitly implied that quantum effects do not qualitatively alter those properties, at the excitation energies which characterize fragmenting nuclei.

The introduction of time-independent stationary descriptions of fragmented systems presupposes that these

^a *carmona@df.unipi.it*

^b *richert@lpt1.u-strasbg.fr*

^c *pierre.wagner@ires.in2p3.fr*

systems are in thermodynamic equilibrium. Whether this is a realistic assumption and is effectively realised is still an open question. There exist however many data which show that most experimental results can be understood in this framework [1].

The present contribution follows a double objective. First, in the framework of lattice models, we want to analyse the effect of the Coulomb interaction which is superimposed onto the short range nearest neighbour interaction which mimics the nuclear potential. This is done in the framework of the so called Ising Model with Fixed Magnetization (IMFM) [9] and its extension to the case where proton-neutron are differentiated from proton-proton and neutron-neutron interactions. The treatment of the long range interaction is performed on the same footing as the short range one i.e. without any approximation in the calculations of the interaction between a given proton and all the others in the system. In a second part we relax the lattice structure of the system. Fragmenting nuclei are disordered systems whose constituents are not located at fixed positions on a regular lattice like in crystals but more in the continuum of position space. A priori, a more realistic description of such systems is realised in the framework of so called cellular models [7]. We show and discuss whether the freedom to occupy any space position leads or not to qualitative changes in the thermodynamic and topological (fragment formation) properties of the system.

In section 2 we present a sketchy description of the IMFM model and the way we implement the Coulomb interaction. We present and discuss the caloric curve, spe-

cific heat and phase diagram for undifferentiated and differentiated protons and neutrons. In this framework we work out the cluster content of the system and related observables for different values of the temperature. Most of the simulations are performed in the framework of the canonical ensemble. A comparison with microcanonical calculations is also presented. In section 3 we introduce the cellular model and study its thermodynamic properties which will be confronted with those obtained with the lattice model. Section 4 is devoted to comments and conclusions.

2 Effect of the Coulomb interaction on finite systems described by Ising-type lattice models

2.1 The models and their implementation

The classical system with A particles located on a cubic lattice with L^3 sites is described by Hamiltonians of the form

$$H = - \sum_{\langle i,j \rangle} V_{K_i K_j} n_i n_j + \frac{1}{2} \sum_{i \neq j} \frac{e^2 Z_i Z_j}{r_{ij}} \quad (1)$$

where K_i ($i = 1, \dots, L^3$) labels either a proton (p) or a neutron (n). The short range potential $V_{K_i K_j}$ acts only between pairs of nearest neighbour particles $\langle i, j \rangle$, when the sites i and j are both occupied ($n_i = n_j = 1$), unoccupied sites correspond to $n_k = 0$. The interaction strengths are chosen in two different ways, either $V_{nn} = V_{pp} = V_{np} = \epsilon = 5$ MeV (undifferentiating potential, case U in the sequel) or $V_{nn} = V_{pp} = 0, V_{np} = \epsilon_{np} = 5.33$ MeV (dif-

ferentiating potential, case D in the sequel). The latter, (r') to a priori more realistic choice has been used by different authors [10–13], the choice of strength is such that the classical ground state energy of finite nuclear systems is reproduced [14].

The Coulomb term in (1) is such that $Z_i = 0$ or 1 if particle i is a neutron or a proton respectively. The distance between particles i and j , r_{ij} , is determined on a lattice in which the distance between sites is fixed to $d = 1.8$ fm.

The canonical partition function reads

$$\mathcal{Z}(\beta) = \sum_{[n_i, Z_i]} e^{-\beta H} \cdot \delta_{\sum_i n_i, A} \cdot \delta_{\sum_i Z_i, Z} \quad (2)$$

where Z is the total number of charges in the system. In the calculations Z/A was fixed at the value of 0.4.

The thermodynamic properties and the space occupation by particles and bound clusters are obtained from realisations generated by means of Metropolis Monte Carlo simulations in which particles are moved on the lattice. Technical details about the algorithm used in the framework of the canonical ensemble have been given elsewhere [9]. We selected 5×10^4 realisations corresponding each to $10 \times L^3$ Metropolis steps.

We have also performed calculations in the framework of the microcanonical ensemble. A given realisation (r) with fixed energy E has a weight

$$W_E(r) \sim (E - U(r))^{\frac{D_A}{2}-1} \cdot \Theta(E - U(r)) \quad (3)$$

where $U(r)$ is the potential energy, Θ is the step function, D the space dimension, here $D = 3$. Detailed balance fixes the acceptance rate from a realisation (r) to a realisation

$$W_{r \rightarrow r'} = \min \left[1, \frac{W_E(r')}{W_E(r)} \right]. \quad (4)$$

The simulations were done with open boundary conditions on the edges of the lattice both in the case of the canonical and microcanonical ensembles.

2.2 Thermodynamics and cluster size distributions

The quantities which we consider here are the caloric curve and the specific heat for fixed volume which in the canonical ensemble reads

$$C_V = \frac{d \langle U \rangle}{dT} = \frac{1}{T^2} (\langle U^2 \rangle - \langle U \rangle^2).$$

The brackets stand for an average over an ensemble of systems. In the microcanonical ensemble the temperature is related to the kinetic energy K of the system by

$$T = 2 \langle K \rangle / AD.$$

Then the specific heat can be cast in the simple form [15]

$$C_V = \frac{DA}{2} \left[\frac{DA}{2} - \left(\frac{DA}{2} - 1 \right) \langle K \rangle \left\langle \frac{1}{K} \right\rangle \right]^{-1} - DA.$$

In the absence of the Coulomb interaction clusters of bound particles are determined in the same way as in ref. [8] by application of the Coniglio-Klein prescription [16] which fixes the condition under which a particle located on a site which is topologically connected to a cluster does effectively belong to this bound cluster. The test between nearest neighbour pairs of particles is made by means of the probability $p = 1 - \exp(-\epsilon/2T)$ in case U , with ϵ replaced by $\epsilon_{pp}, \epsilon_{nn}, \epsilon_{np}$ in case D, depending on

the nature of the particles which are involved. The probability p is then compared to a random number $\xi \in [0, 1]$. If $\xi \leq p$ the particles are considered as being bound, if $\xi > p$ they are not.

The Coulomb interaction is taken into account in the case U and for a pair of neighbouring charged particles by replacing ϵ by $\epsilon - e^2/d$ where d is the (fixed) distance between the particles. In the case D p is not modified since neighbouring charged particles are not bound $\epsilon_{pp} = 0$.

The cluster size distribution can be determined for any fixed density $\rho = A/L^3$ and temperature T . From its knowledge one can work out different observables. Here we restrict ourselves to the behaviour of the largest cluster A_{max} as a function of $\log S_2$, with $S_2 = m_2/m_1$ and m_k the k^{th} moment of the distribution [17, 18].

2.3 Effect of the Coulomb interaction on the thermodynamic properties of the system

The effect of the Coulomb interaction has been studied in both cases U and D with the two-body strengths given in 2.1. Fig. 1 shows the caloric curve and the specific heat associated to a system with $L = 10$ and $\rho = 0.3$ for case U. Calculations have been performed in both the canonical and microcanonical framework. As it can be seen in Fig. 1, on the specific heat, the results are undistinguishable. The point of interest is the fact that the Coulomb interaction induces a sizable shift in the energy for fixed temperature on the caloric curve which increases approximately parallel to each other and a reduction of about 1.5 MeV in the temperature corresponding to the maximum of C_V .

This behaviour is general, whatever the size of the system and its density. The expected drop in the temperature in the presence of Coulomb reflects also in the (ρ, T) phase diagram shown in Fig. 2, in which the coexistence line has been fixed by following the maximum of C_V . One may mention the slight dissymmetry with respect to $\rho = 0.5$. For larger ρ the Coulomb effect is larger than for small densities and consequently produces a stronger shift in the temperature which defines the border of the coexistence region. This is due to the fact that higher ρ corresponds to stronger packing, hence charges interact more effectively. In case D, when the particles are differentiated, the results are qualitatively similar for both the caloric curve and the specific heat with a similar shift of 1.5 MeV in the temperature, see Fig. 3. In this case, the maximum of C_V is much more damped when Coulomb is present than in case U, and the transition region is therefore less precisely defined.

Notice that in both cases the caloric curve shows the characteristic behaviour of a system which undergoes a continuous transition. This is also the case in a microcanonical calculation. Comments and discussions about this point have been made in ref. [19].

2.4 The effect of the Coulomb interaction on the cluster size distributions and related observables

The behaviour of the mass distribution of clusters is shown in Fig. 4 for case D, temperatures lie in the range 3 – 5 MeV. One observes again a shift in the behaviour of the system when the Coulomb interaction is switched

on. For the same temperature, the distribution without Coulomb contains more larger clusters. This is understandable since the long range interaction is repulsive and tends to split the bond fragments. The whole picture is also consistent with the thermodynamic behaviour of the system. This is seen in Fig. 2 on the line which separates the heavy cluster behaviour below the line from the light cluster behaviour above it and stands as the finite size remnant of a continuous set of transition points in the percolation framework [20]. Indeed, the line lies at lower temperatures when the Coulomb interaction is present. Notice that this separation line (Kertész line) does not end at $\rho = 0.5$ as expected in the lattice gas model [8].

This may have several origins, the finite size of the system, the determination of the coexistence line, the determination of the location of the cluster separation line which is fixed by the maxima of the second moment m_2 of the mass distribution with respect to the temperature for fixed ρ .

Fig. 5 shows the correlation between A_{max} and S_2 in case D. Events which come at large A_{max} correspond to the presence of heavy clusters, those with small A_{max} to the presence of many small clusters. The intermediate region shows events which correspond to the transition region in the percolation framework. As it can be seen, this region appears again for lower temperatures in the case where the Coulomb interaction is acting.

A further observable of physical interest which can be experimentally determined is the ratio of the number of neutrons to the number of protons, N/Z , which are present in the clusters [21]. Fig. 6 shows the evolution of

this ratio for clusters of mass $A = N + Z \geq 40$ with increasing temperature for case D. One observes a decrease of the relative number of neutrons, both in the absence and the presence of the Coulomb interaction. This is in agreement with the results of ref. [13] and, for heavy clusters, with the experimental results of ref. [22]. The decrease is apparently slightly more pronounced in the case where the Coulomb interaction is active, although, as indicated, the fluctuations from event to event increase with increasing temperature. This result may appear to be somewhat paradoxical. It may be due to the fact that for fixed temperature the cluster size distribution is different in both cases as we already saw above.

Finally, the evolution of the N/Z ratios with the mass is shown in Figs. 7 for case D. In Fig. 7a the results correspond to the case where the Coulomb interaction is included. The ratio drops from $N/Z \sim 1.6$ for $A = 3$ to 1.2 for the largest masses. A similar behaviour is observed in Fig. 7b for a higher temperature and in the absence of the Coulomb interaction. Hence lighter species are more neutron rich than heavier ones. This fact which has already been observed in the calculations of ref. [13] in the absence of the Coulomb interaction remains valid when Coulomb is present and seems to be in agreement with the experimental findings [23, 24].

3 Cellular model approach to the description of fragmenting nuclei

A system of A particles is contained in a cube of volume V in $3D$ space and divided into cells of volume d^3 , $V = L^3 d^3$. Cells are either empty or occupied by at most one particle characterized by its random position \mathbf{r}_i ($i = 1, \dots, A$) in the cell and random momentum \mathbf{p}_i [7]. The particles are classical. Neighbouring particles interact through a short range two-body potential $V_0(r_{ij})$ which is repulsive at short distance and attractive for $r_{ij} \geq 1.55$ fm [25]. In the calculations $d = 1.8$ fm. The Coulomb interaction is not taken into account. The Hamiltonian is written as

$$H = \sum_{i=1}^A \frac{p_i^2}{2m} - \sum_{\langle ij \rangle} V_0(r_{ij}) n_i n_j \quad (5)$$

with $n_i = 0(1)$ if the cell i is empty (occupied).

Similarly to the lattice case we have worked out the thermodynamic properties of such a system in the framework of both the canonical and microcanonical ensemble. The generation of configurations by means of a Metropolis Monte Carlo procedure is performed in the following way. Starting from an initial configuration in which the particles are disposed randomly into the available cells one performs either the move of a particle into an empty cell, or changes the position of a particle in its cell. Each operation is performed with a probability $1/2$, the application of the Metropolis Monte Carlo algorithm leads to a minimum in energy in the framework of the canonical ensemble. In the case of the microcanonical ensemble the test is the one described in section 2.1, Eq. (4).

Typical results can be seen on Fig. 8 which shows the caloric curve and the specific heat. Both ensembles lead to a very close behaviour of these quantities. This behaviour is qualitatively similar to those obtained with lattice models. The same is true for the corresponding phase diagram shown in Fig. 9. The present calculations have been performed for a fixed volume with 8^3 sites and the possible transition looks continuous in this case. The small depression for $\rho = 0.5$ reminds the same effect which was found in the IMFM calculations of ref. [9]. The dotted line shows the separation line of heavy and light clusters as in the case of the lattice models. Its behaviour is very similar to the one observed in Fig. 2. The fact that its lower end does not coincide with $\rho = 0.5$ may have the same reasons than those presented in section 2.4.

4 Summary and conclusions

In the present work we aimed to present and discuss two points related to the description of nuclear fragmentation by means of microscopic classical models.

We first looked for the effects induced by the long range Coulomb interaction which acts between charged particles in the presence of a short range attractive potential mimicking the nuclear interaction. We have shown on a lattice model that the Coulomb interaction does not induce any qualitative change in the thermodynamics and cluster size distribution in the different phases in which the system exists. The essential quantitative effect is a global systematic and sizable shift of the temperature of the system by about 1.5 MeV in the models which have been worked out

both in the thermodynamic and cluster transitions. The same type of effect has already been mentioned in former studies [26]. We have also investigated the behaviour of the cluster content, both in the absence and presence of the Coulomb interaction.

In a second part we introduced a cellular model aimed to describe a disordered system of particles in thermodynamic equilibrium in the framework of the canonical and microcanonical ensembles. The results show that such models, though a priori more realistic than lattice models, are descriptions which lead qualitatively to the same properties, at least when finite systems are concerned. This leads to the conclusion that lattice models which are simple to handle should be good enough for a schematic description of nuclear fragmentation processes if the generated systems are in thermodynamic equilibrium. There remains however the problem concerning the importance of quantum effects. These may be the weaker the higher the temperature, but this point has to be confirmed.

References

1. See f.i. J. Richert and P. Wagner, nucl-th/0009023, Phys. Rep. (to be published).
2. T.D. Schultz, D.C. Mattis and E.H. Lieb, Rev. Mod. Phys. **36**, 856 (1964).
3. R.B. Potts, Proc. Camb. Phil. Soc. **48**, 106 (1952).
4. S.K. Samaddar and J. Richert, Z. Phys. A **332**, 443 (1989).
5. S.K. Samaddar and J. Richert, Phys. Lett. B **218**, 381 (1989).
6. S. Das Gupta and Jicai Pan, Phys. Rev. C **53**, 1319 (1996) and refs. therein.
7. B. Elattari, J. Richert, P. Wagner and Y.M. Zheng, Nucl. Phys. A **592**, 385 (1995).
8. X. Campi and H. Krivine, Nucl. Phys. A **620**, 46 (1997).
9. J.M. Carmona, J. Richert and A. Tarancón, Nucl. Phys. A **643**, 115 (1998).
10. J. Borg, I.N. Mishustin and J.P. Bondorf, Phys. Lett. B **470**, 13 (1999).
11. Ph. Chomaz, V. Duflot and F. Gulminelli, Phys. Rev. Lett. **85**, 3587 (2000) and refs. therein.
12. J. Pan and S. Das Gupta, Phys. Rev. C **57**, 1839 (1998).
13. Ph. Chomaz and F. Gulminelli, Phys. Lett. B **447**, 221 (1999).
14. R.J. Lenk, T.J. Schlagel and V.R. Pandharipande, Phys. Rev. C **42**, 372 (1990).
15. J.R. Ray and C. Freléchoz, Phys Rev. E **53**, 3402 (1996).
16. A. Coniglio and W. Klein, J. Phys. A **13**, 2775 (1980).
17. X. Campi, J. Phys. A: Math. Gen. **19**, L917 (1986).
18. X. Campi, Phys. Lett. B **208**, 351 (1988).
19. J.M. Carmona, N. Michel, J. Richert and P. Wagner, Phys. Rev. C **61**, 37304 (2000).
20. D. Stauffer and A. Aharony, *Percolation Theory*, Taylor and Francis eds., 1994.
21. J. Pochodzalla and W. Trautmann, nucl-ex/0009016.
22. P.M. Milazzo, A.S. Botvina, G. Vannini, N. Colonna, F. Gramegna, G.V. Margagliotti, P.F. Mastinu, A. Moroni and R. Rui, Phys. Rev. C**62**, 041602(R) (2000).
23. S.J. Yennello et al., Phys. Lett. B **321**, 15 (1994); H. Johnston et al., Phys. Lett. B **371**, 186 (1996).
24. H.S. Xu et al., Phys. Rev. Lett. **85**, 716 (2000).

25. L. Wilets, E.M. Henley, M. Kraft and A.D. McKellar, Nucl.

Phys. A **282**, 341 (1977).

26. T.S. Biró, J. Knoll and J. Richert, Nucl. Phys. A **459**, 692

(1986).

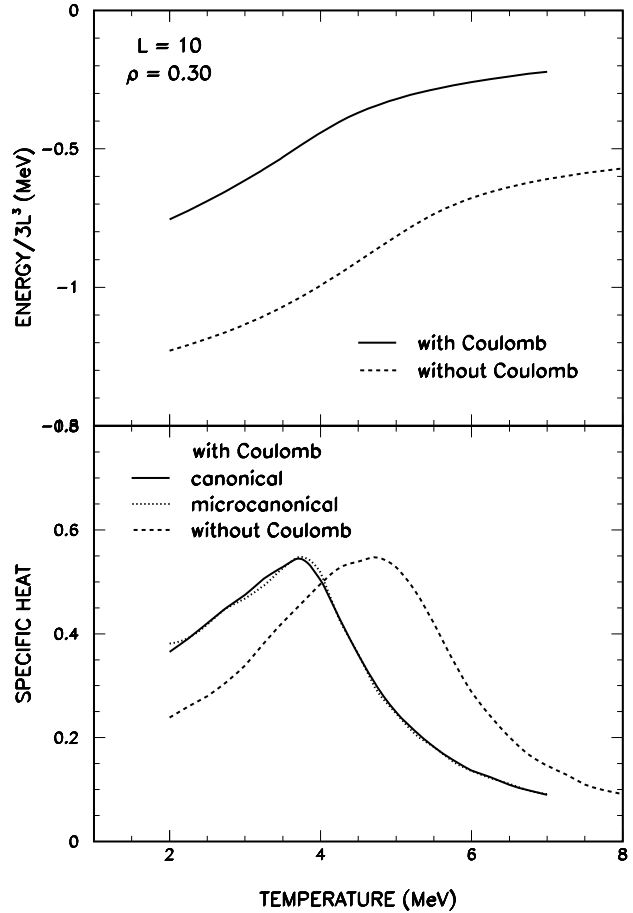


Fig. 1. Caloric curves and specific heat for a lattice model with $A = 300$ undifferentiated particles (protons and neutrons) in a volume $L^3 = 10^3$. Full and open lines correspond respectively to results including or not the Coulomb interaction. The specific heat calculated with the Coulomb interaction in the framework of the microcanonical ensemble is represented by a dotted line.

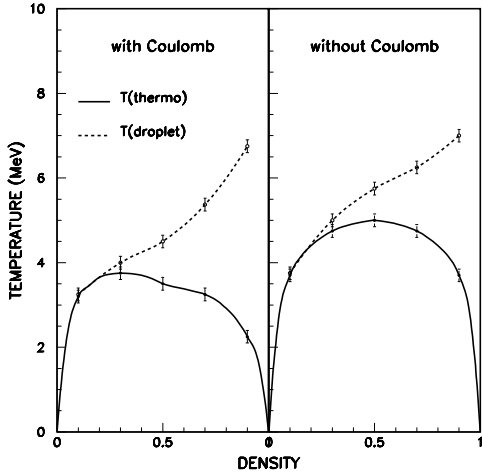


Fig. 2. Phase diagrams (ρ, T) with Coulomb interaction (left) and without Coulomb interaction (right) for undifferentiated particles. The full line indicates the phase separation, the dashed line the separation line between systems with heavy clusters (below) and light clusters and particles (above). See text.

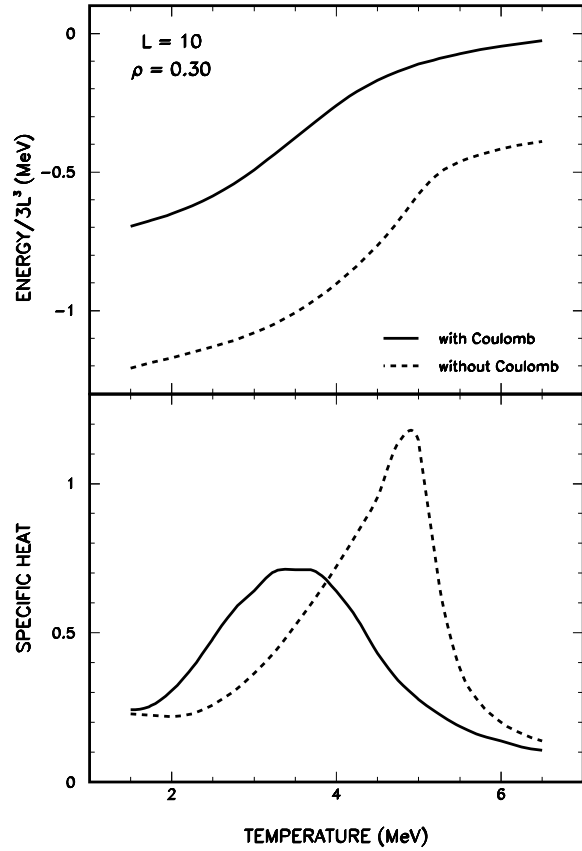


Fig. 3. Same as Fig. 1 for differentiated particles (protons and neutrons). Calculations are done in the canonical ensemble.

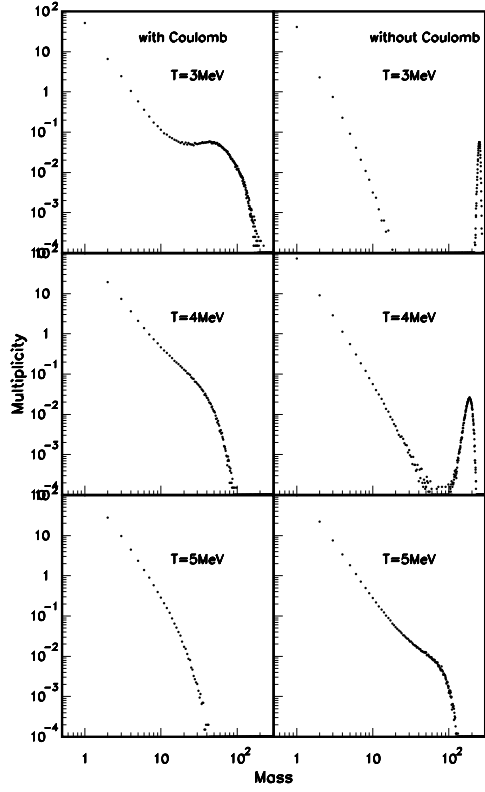


Fig. 4. Cluster size multiplicities for different temperatures. Left column: with Coulomb interaction. Right column: without Coulomb interaction. See text.

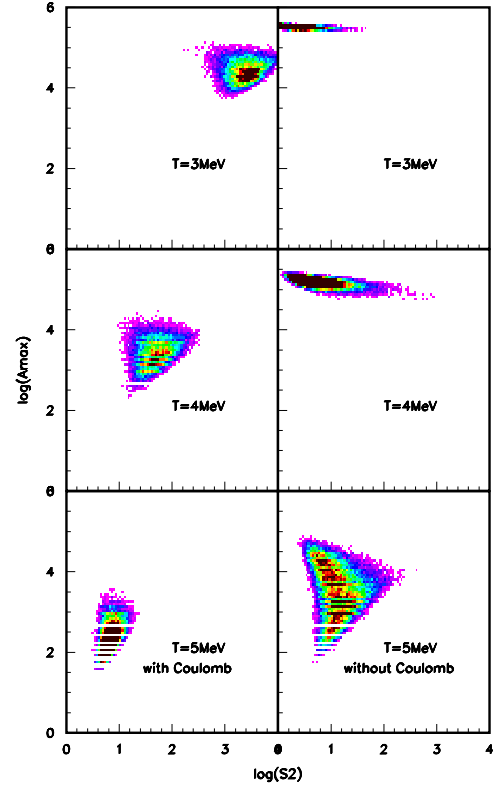


Fig. 5. Size of the heaviest cluster A_{max} vs. $S_2 = m_2/m_1$ represented for the different Monte Carlo events. m_2 and m_1 are the second and first moments of the cluster size distribution.

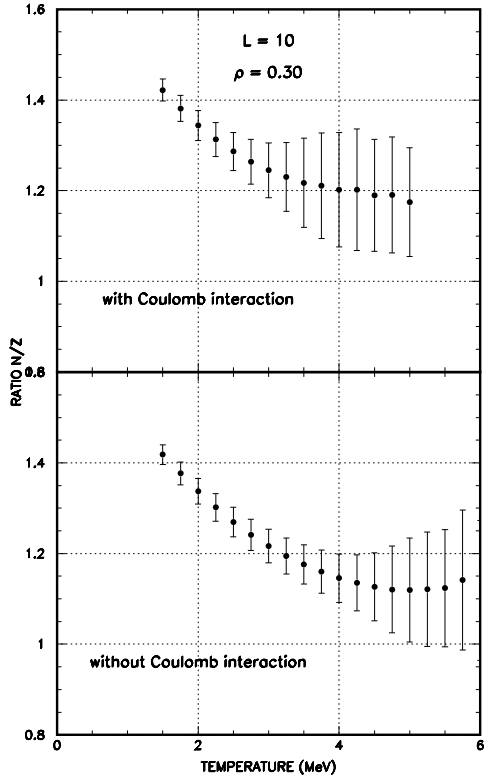


Fig. 6. Average isotopic ratios N/Z and fluctuations widths in the clusters as a function of the temperature in the absence and presence of the Coulomb interaction. Volume $L^3 = 10^3$, density $\rho = 0.3$. See comments in the text.

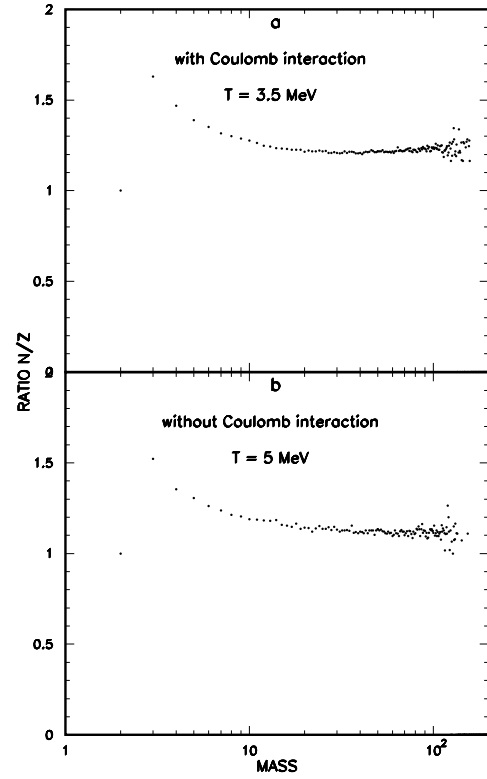


Fig. 7. Isotopic ratios N/Z in the clusters as a function of the cluster size. Upper part (a): without Coulomb interaction. Lower part (b): with Coulomb interaction.

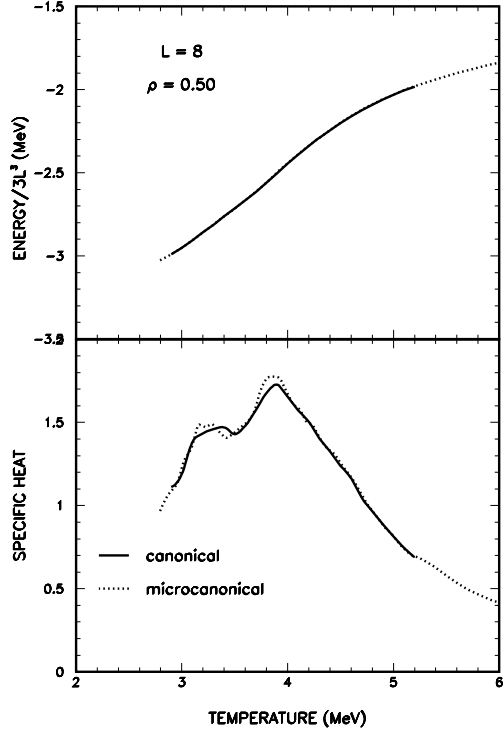


Fig. 8. Canonical and microcanonical caloric curves and specific heat in the framework of the cellular model for a system of $A = 256$ particles in a volume $L^3 = 8^3$. See comments in the text.

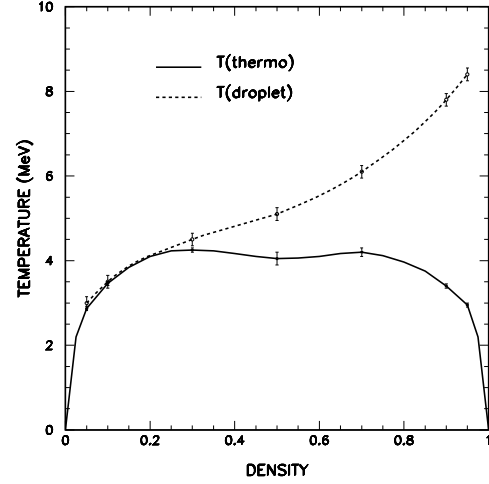


Fig. 9. Phase diagrams (ρ, T) in the framework of the cellular model for a system with $A = 256$ particles in a volume $L^3 = 8^3$. The dashed line has the same meaning as in Fig. 2.